# Modeling uncertainties for local nonlinearities: application to the drill-string dynamics

T.G. Ritto, Christian Soize, R. Sampaio

COMPDYN 2009
ECCOMAS Thematic Conference on
Computational Methods in Structural Dynamics and Earthquake Engineering
M. Papadrakakis, N.D. Lagaros, M. Fragiadakis (eds.)
Rhodes, Greece, 22-24 June 2009

# MODELING UNCERTAINTIES FOR LOCAL NONLINEARITIES: APPLICATION TO THE DRILL-STRING DYNAMICS

**T. G. Ritto [1,2], C. Soize [2] and R. Sampaio[1]**

[1]Mechanical Engineering Department – PUC-Rio
Rua Marquês de São Vicente, 225, Gávea, RJ, CEP: 22453-900, Brazil,
e-mail: thiagoritto@gmail.com, rsampaio@puc-rio.br

[2] Université Paris-Est, Laboratoire de Modélisation et Simulation Multi Echelle, MSME FRE3160 CNRS
5 bd Descartes, 77454 Marne-la-Vallée, France
e-mail: christian.soize@univ-paris-est.fr

**Keywords:** probabilistic model, local nonlinearities, nonlinear stochastic dynamics, drill-string dynamics, bit-rock stochastic model.

**Abstract.** *A probabilistic model is proposed to model uncertainties for local nonlinearities. The model is applied to a slender structure that turns and drills into rocks in search of oil, called drill-string, in which the local nonlinearity is the bit-rock interaction. The Maximum Entropy Principle is used to construct a probabilistic model for the nonlinear operator related to the bit-rock interaction model. A numerical model is developed using the Timoshenko beam theory and it is discretized by means of the Finite Element Method. The nonlinear dynamics analyzed considers a imposed rotation at the top, weight-on-hook, a fluid-structure interaction (that takes into account the drilling fluid that flows downwards the column and upwards the annulus), impact and rubbing between the column and the borehole, and finite strains (what couples axial, torsional and lateral vibrations). The development presented corresponds to a new approach to take into account model uncertainties in local nonlinearities using a probabilistic approach.*

## 1 INTRODUCTION

In this work the drill-string problem is used to show an approach to take into account uncertainties in a local nonlinearity which, for the system considered, is the bit-rock interaction. Previous works have studied a stochastic modeling for local uncertainties in linear dynamical systems, as, for instance, boundary conditions [9] and coupling [10]. Specifically in [9, 10], a nonparametric probabilistic approach [19] was employed so that both data and model uncertainties could be taken into account. The aim and novelty of this paper is to model uncertainties in a local nonlinearity using the nonparametric probabilistic approach.

Drill-strings are slender structures used to dig into the rock in search of oil. The drill-string dynamics must be controlled to avoid failures [8], see a general vibration perspective of the oil and gas drilling process in [23]. We consider a vertical well for which the length of the column may reach some kilometers. The drill-string is composed by thin tubes called drill-pipes and some thicker tubes called drill-collars. The thicker tubes are in the bottom region which is known as the Bottom-Hole-Assembly (BHA). Figure 1 shows the general scheme of the system analyzed. The forces taking into account are: the motor torque (as a constant rotation speed at the top $\Omega_x$); a constant supporting force $f_{hook}$; the torque $t_{bit}$ and force $f_{bit}$ at the bit; the weight of the column; the fluid forces; the impact and rubbing between the column and the borehole; the forces due to the stabilizer; plus the elastic and kinetic forces due to the deformation and to the motion of the structure.

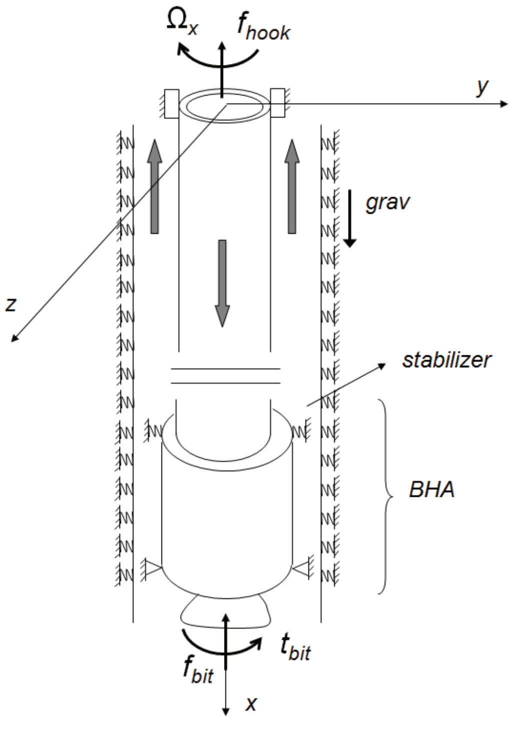


Figure 1: General scheme.

In the literature, the nonlinear dynamics of a drill-string is modeled in several different ways, *e.g.*[2, 26, 7, 25, 16]. These models are able to quantify some effects that occur in a drilling operation, as the stick-slip oscillations, for instance, but they cannot correctly predict the dynamic response of a real system. This is explained, first, because the above models are too simple compared to the real system and, second, because the uncertainties are not taken into account.

Moreover, a fluid-structure interaction that takes into account the drilling fluid that flows inside and outside the column is not considered in any of the above mentioned works. This kind of fluid-structure interaction model was proposed in [12] for a plane problem in another context, and it was extended for our problem [14]. To model the column, the Timoshenko beam model is employed and the Finite Element Method is used to discretize the system. Besides, it is considered: finite strain with no simplifications (higher order terms are not neglected); quadratic terms derived from the kinetic energy; impact and rubbing between the column and the borehole; stabilizers; fluid-structure interaction; and a bit-rock interaction that models how the bit penetrates the rock.

The uncertainty analysis of this paper is focused on the bit-rock interaction because it is a local nonlinearity and one of the most important sources of uncertainties of this problem. A probabilistic approach is used to model the uncertainties in the nonlinear operator.

The bit-rock interaction model chosen was the one developed in [26] basically for two reasons: (1) it is able to reproduce the main phenomena (as stick-slip oscillations); (2) it describes well the penetration of the bit into the rock (so we can analyze the rate-of-penetration-ROP). Usually the bit is considered fixed, [7, 16], or an average rate of penetration is assumed, [2].

The nonparametric probabilistic approach [19, 20, 21] is used to model the uncertainties in the bit-rock interaction which is represented by a nonlinear operator. Note that a new strategy has to be developed to take into account uncertainties in a local nonlinear operator. The probability density function is derived using the Maximum Entropy Principle [18, 5, 6]. Two probabilistic models are analyzed: one that allows only change in the parameters (called noncoupled model) and another that permits changes in the model (the usual nonparametric model). Then, by perturbing the bit-rock operator, the robustness of the models used is analyzed.

The paper is organized as following. In Section 2 the mean model is presented and in Section 3 the probabilistic model of the bit-rock interaction model is developed. The numerical results are shown in Section 4 and the concluding remarks are made in Section 5.

## 2 MEAN MODEL

In this Section the equations used to model the problem are presented. The Total Lagrangian (TL) formulation is used, six degrees of freedom are considered in the points of discretization (three translations, $u$, $v$ and $w$, and three rotations $\theta_x$, $\theta_y$ and $\theta_z$), the stress tensor is the second Piola-Kirchhoff tensor and finite strains are considered (Green-Lagrange strain tensor). The main hypothesis are the following: (1) the drill-string is axisymmetric about $x$-axis; (2) the following strain components are neglected: $e_{yy} \sim e_{zz} \sim \gamma_{yz} \sim \gamma_{zy} \sim 0$; (3) the rotations $\theta_y$ and $\theta_z$ are small, i.e, $\sin(\theta_y) \sim \theta_y$, $\sin(\theta_z) \sim \theta_z$ and $\cos(\theta_y) \sim \cos(\theta_z) \sim 1$; (4) the stress-strain relationship is linear; and (5) the rotation $\theta_x$ is finite (the rotational speed $\dot{\theta}_x$, of course, is not constant over the element).

The strategy used in this work is, in some respects, similar to the one used in [7], but there are several important additional features, such as (1) impact and rubbing between the column and the borehole; (2) shear (Timoshenko beam model); (3) finite $\theta_x$; (4) fluid-structure interaction; (5) all the terms of the strain energy are used in the analysis; (5) a bit-rock interaction model that allows the simulation of the bit penetration is used; and (6) constant force at the top (supporting force or weight-on-hook).

To derive the dynamic equations, the extended Hamilton Principle is used. Defining the potential $\Pi$ by

$$\Pi = \int_{t_1}^{t_2} (U - T - W)dt \,, \tag{1}$$

where $U$ is the potential strain energy, $T$ is the kinetic energy and $W$ is the work done by the nonconservative forces and by any force not accounted for in the potential energy. The first variation of $\Pi$ must vanish

$$\delta\Pi = \int_{t_1}^{t_2} (\delta U - \delta T - \delta W)dt = 0 \,. \tag{2}$$

### 2.1 General equations

In the discretization by means of the Finite Element Method, a two-node approximation with six degrees of freedom per node is chosen. The nodal displacement is written as

$$u_e = \mathbf{N}_u \mathbf{u}_e \quad , \quad v_e = \mathbf{N}_v \mathbf{u}_e \quad , \quad w_e = \mathbf{N}_w \mathbf{u}_e \,, \tag{3}$$

$$\theta_{xe} = \mathbf{N}_{\theta_x} \mathbf{u}_e \quad , \quad \theta_{y_e} = \mathbf{N}_{\theta_y} \mathbf{u}_e \quad , \quad \theta_{ze} = \mathbf{N}_{\theta_z} \mathbf{u}_e \,, \tag{4}$$

where $\mathbf{N}$ are the shape functions (see [14]); $u_e$, $v_e$ and $w_e$ are the displacements in $x$, $y$ and $z$ directions; $\theta_{xe}$, $\theta_{ye}$ and $\theta_{ze}$ are the rotations about $x$, $y$ and $z$ axis. The element coordinate is $\xi = x/l_e$, and

$$\mathbf{u}_e = \begin{pmatrix} u_1 & v_1 & \theta_{z1} & w_1 & \theta_{y_1} & \theta_{x1} & u_2 & v_2 & \theta_{z2} & w_2 & \theta_{y_2} & \theta_{x2} \end{pmatrix}^T \,, \tag{5}$$

where $(\cdot)^T$ means transpose. After assemblage, the final discretized system is written as

$$([M] + [M_f])\ddot{\mathbf{u}} + ([C] + [C_f])\dot{\mathbf{u}} + ([K] + [K_f])\mathbf{u} = \mathbf{f}_{NL}(t, \mathbf{u}, \dot{\mathbf{u}}, \ddot{\mathbf{u}}) + \mathbf{f}_c + \mathbf{f}_g + \mathbf{f}_f \,. \tag{6}$$

Where $\mathbf{u}$ is the $\mathbb{R}^m$-valued response for which $m$ is the number of degrees of freedom of the system. $[M]$, $[C]$ and $[K]$ are the usual mass, damping and stiffness matrices; $[M_f]$, $[C_f]$, $[K_f]$ are the added fluid mass, damping and stiffness matrices, and $\mathbf{f}_f$ is the fluid force vector; $\mathbf{f}_g$ is the gravity force; $\mathbf{f}_c$ is a concentrated reaction force at the bit; $\mathbf{f}_{NL}(t, \mathbf{u}, \dot{\mathbf{u}}, \ddot{\mathbf{u}})$ is the nonlinear force vector that is decomposed in

$$\mathbf{f}_{NL}(t, \mathbf{u}, \dot{\mathbf{u}}, \ddot{\mathbf{u}}) = \mathbf{f}_{ke}(\ddot{\mathbf{u}}, \dot{\mathbf{u}}, \mathbf{u}) + \mathbf{f}_{se}(\mathbf{u}) + \mathbf{f}_{ip}(\mathbf{u}) + \mathbf{f}_{br}(\dot{\mathbf{u}}) + \mathbf{g}(t) \,. \tag{7}$$

where $\mathbf{f}_{ke}(\mathbf{u}, \dot{\mathbf{u}}, \ddot{\mathbf{u}})$ is composed by the quadratic terms of the kinetic energy; $\mathbf{f}_{se}(\mathbf{u})$ is composed by the quadratic and higher order terms of the strain energy; $\mathbf{f}_{ip}(\mathbf{u})$ are the forces due to the impact and rubbing between the column and the borehole; $\mathbf{f}_{br}(\dot{\mathbf{u}})$ are the forces due to the bit-rock interactions, see section 2.3; and $\mathbf{g}(t)$ is the force that corresponds to the Dirichlet boundary condition (rotation imposed at the top). For a detailed explanation of each term of the nonlinear force see [14].

The dynamics is computed from a prestressed configuration, $\mathbf{u}_S = [K]^{-1}(\mathbf{f}_g + \mathbf{f}_c + \mathbf{f}_f)$, then Eq. (6) becomes

$$([M] + [M_f])\ddot{\bar{\mathbf{u}}} + ([C] + [C_f])\dot{\bar{\mathbf{u}}} + ([K] + [K_f] + [K_g(\mathbf{u}_S)])\bar{\mathbf{u}} = \bar{\mathbf{f}}_{NL}(t, \bar{\mathbf{u}}, \dot{\bar{\mathbf{u}}}, \ddot{\bar{\mathbf{u}}}) \,, \tag{8}$$

in which $\bar{\mathbf{u}} = \mathbf{u} - \mathbf{u}_S$ and $\mathbf{f}_{se}(\mathbf{u})$ was split in $\bar{\mathbf{f}}_{se}(\bar{\mathbf{u}})$ and $[K_g(\mathbf{u}_S)]\bar{\mathbf{u}}$, where $[K_g(\mathbf{u}_S)]$ is the geometric stiffness matrix.

### 2.2 Fluid-structure interaction

The drilling fluid (mud) is responsible to transport the cuttings (drilled solids) from the bottom to the top to avoid clogging of the hole. It also plays an important role in cooling and stabilizing the system [1]. The rheological properties of the mud are complexes, see [3] for instance. There is no doubt that the drilling fluid influences the dynamics of a drill-string, but to solve the complete problem would be too expensive computationally. There are some works that study only the drilling fluid flow, as, for example, [4, 13]. In this work a linear fluid-structure coupling model similar to [12] is used. In this simplified model there are the following hypotheses,

1. The inside fluid is inviscid, while the outside flow is viscous.
2. The flow induced by the rotation speed about $x$-axis is not considered in the analysis.
3. The pressure varies linearly with $x$.
4. The fluid is added in the formulation as a constant mass matrix $[M_f]$, a constant stiffness matrix $[K_f]$, a constant damping matrix $[C_f]$ and a constant force $\mathbf{f}_f$ (see Eq. (9)).

For short, the element equations are presented. These equations are an extension and an adaptation of the model developed in [12].

$$
\begin{aligned}
[M_f]^{(e)} &= \int_0^1 (M_f + \chi\rho_f A_o)\,(\mathbf{N}_w^T\mathbf{N}_w + \mathbf{N}_v^T\mathbf{N}_v) l_e d\xi\,,\\
[K_f]^{(e)} &= \int_0^1 \left(-M_f U_i^2 - A_i p_i + A_o p_o - \chi\rho_f A_o U_o^2\right)(\mathbf{N'}_w^T\mathbf{N'}_w + \mathbf{N'}_v^T\mathbf{N'}_v)\frac{1}{l_e}d\xi +\\
&\quad + \int_0^1 \left(-A_i\frac{\partial p_i}{\partial x} + A_o\frac{\partial p_o}{\partial x}\right)(\mathbf{N}_{\theta_y}^T\mathbf{N}_{\theta_y} + \mathbf{N}_{\theta_z}^T\mathbf{N}_{\theta_z}) l_e d\xi\,,\\
[C_f]^{(e)} &= \int_0^1 (-2M_f U_i + 2\chi\rho_f A_o U_o)\,(\mathbf{N}_{\theta_y}^T\mathbf{N}_{\theta_y} + \mathbf{N}_{\theta_z}^T\mathbf{N}_{\theta_z}) l_e d\xi +\\
&\quad + \int_0^1 \left(\frac{1}{2}C_f\rho_f D_o U_o + k\right)(\mathbf{N}_w^T\mathbf{N}_w + \mathbf{N}_v^T\mathbf{N}_v) l_e d\xi\,,\\
\mathbf{f}_f^{(e)} &= \int_0^1 \left(M_f g - A_i\frac{\partial p_i}{\partial x} - \frac{1}{2}C_f\rho_f D_o U_o^2\right)\mathbf{N}_u^T l_e d\xi\,.
\end{aligned}
\tag{9}
$$

in which,

$M_f$ is the fluid mass per unit length,
$\rho_f$ is the density of the fluid,
$\chi = \dfrac{(D_{ch}/D_o)^2 + 1}{(D_{ch}/D_o)^2 - 1} \quad (> 1)$,
$D_{ch}$ is the borehole (channel) diameter,
$D_i, D_o$ are the inside and outside diameters of the column,
$U_i, U_o$ are the inlet and outlet flow velocities,

$p_i, p_o$ are the pressures inside and outside the drill-string,
$A_i, A_o$ are the inside and outside cross sectional area of the column,
$C_f, k$ are the fluid viscous damping coefficients.

It is assumed that the inner and the outer pressures ($p_i$ and $p_o$) vary linearly with $x$

$$p_i = (\rho_f g)\, x + p_{cte}\,, \tag{10}$$

$$p_o = \left(\rho_f g + \frac{F_{fo}}{A_o}\right) x\,, \tag{11}$$

where $p_{cte}$ is a constant pressure and $F_{fo}$ is the friction force due to the external flow given by

$$F_{fo} = \frac{1}{2} C_f \rho_f \frac{D_o^2 U_o^2}{D_h}\,. \tag{12}$$

In the above equation, $D_h$ is the hydraulic diameter (=$4A_{ch}/S_{tot}$) and $S_{tot}$ is the total wetted area per unit length ($\pi D_{ch} + \pi D_o$). Note that the reference pressure is $p_o|_{x=0} = 0$. Another assumption is that there is no head loss when the fluid passes from the drill-pipe to the drill-collar (and vice-versa). The head loss due to the change in velocity of the fluid at the bottom (it was going down, then it goes up) is given by

$$h = \frac{1}{2g}(U_i - U_o)^2\,. \tag{13}$$

Note that if the geometry and the fluid characteristics are given, only the inlet flow at $x = 0$ can be controlled because the fluid speed is calculated using the continuity equation and the pressures are calculated using the Bernoulli equation.

Examining Eq. (9), it can be seen that the mass matrix due to the fluid is the usual added mass that, in our case, represents a significative part of the total mass (in norm). For example, using representative values (used in our simulations), the added mass is around 50%, what changes the natural frequencies in about 20%.

The stiffness matrix due to the fluid depends on the speed of the inside and outside flow, on the pressure and on the pressure derivatives. Analyzing the signs in the equation (Eq. 9) it can be seen see that the outsize pressure tends to stabilize the system while the inside pressure and the flow tends to destabilize the system. The term $(-p_i A_i + p_o A_0)$ plays a major role on the stiffness of the system because, even though $p_i$ is close to $p_o$, in the drill collar region (in the bottom) $A_0$ is around ten times $A_i$ what turns the system stiffer at the bottom.

The damping matrix due to the fluid depends on the flow velocity as well as in the viscous parameter of the fluid, which are not well established values. There are uncertainties to determine the damping characteristics and a stochastic model should be developed to the damping, but in this work a detailed analysis will not be addressed. Finally, the force vector ($\mathbf{f}_f$) represents the buoyancy induced by the fluid and it is the only force in the axial direction ($x$-direction).

### 2.3 Bit-rock interaction

The model used in this work is the one developed by [26], which can be written as

$$\begin{aligned} \dot{u}_{bit} &= -a_1 - a_2 f_{xbit} + a_3 \dot{\theta}_{bit} \\ t_{xbit} &= -\text{DOC}\, a_4 - a_5 \\ \text{DOC} &= \frac{\dot{u}_{bit}}{\dot{\theta}_{bit}} \quad , \end{aligned} \tag{14}$$

where $f_{xbit}$ is the axial force (also called weight-on-bit), $t_{xbit}$ is the torque about $x$-axis and $a_1, \ldots, a_5$ are positive constants that depend on the bit and rock characteristics as well as on the weight-on-bit. Note that $\dot{u}_{bit}$ (=ROP) depends linearly on $f_{xbit}$ and on $\dot{\theta}_{bit}$ (=$\omega_{bit}$), and $t_{xbit}$ depends linearly on the depth-of-cut (DOC). Equation (14) is rewritten as

$$\begin{aligned} f_{xbit} &= -\frac{\dot{u}_{bit}}{a_2 Z(\dot{\theta}_{bit})^2} + \frac{a_3 \dot{\theta}_{bit}}{a_2 Z(\dot{\theta}_{bit})} - \frac{a_1}{a_2} \\ t_{xbit} &= -\frac{\dot{u}_{bit} a_4 Z(\dot{\theta}_{bit})^2}{\dot{\theta}_{bit}} - a_5 Z(\dot{\theta}_{bit}) \end{aligned} \tag{15}$$

where $Z(\dot{\theta}_{bit})$ is the regularization function so that when $\dot{\theta}_{bit}$ approaches to zero $t_{xbit}$ and $\dot{u}_{bit}$ vanish. The regularization function is plotted in Fig. 2(a).

$$Z(\dot{\theta}_{bit}) = \frac{\dot{\theta}_{bit}}{\sqrt{(\dot{\theta}_{bit})^2 + e^2}} \,. \tag{16}$$

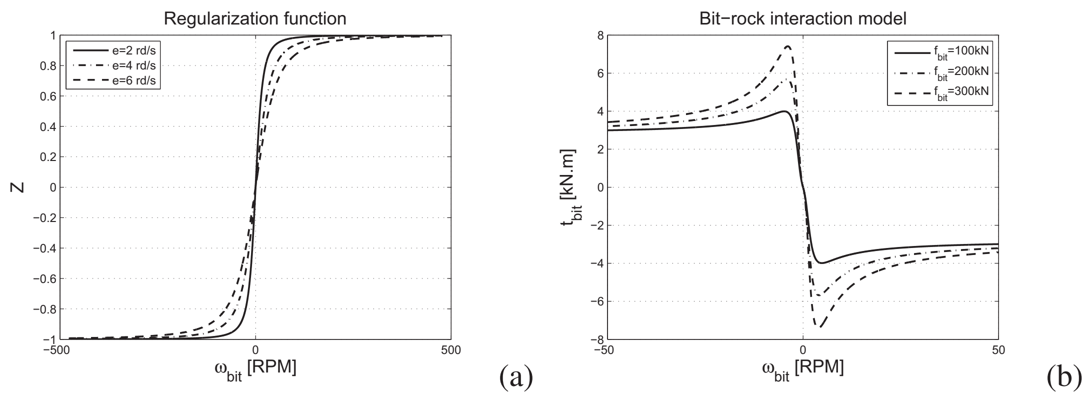


Figure 2: Regularization function (a) and torque at the bit in function of $\omega_{bit} = \dot{\theta}_{bit}$ (b).

Equation (15) was derived in a stable operation with $\dot{\theta}_{bit} \sim 100$ RPM and with $f_{xbit} \sim 100$ kN. In this model the bit exerts only an axial force ($f_{xbit}$) and a torque ($t_{xbit}$) about $x$-axis (see how the torque varies with $\dot{\theta}_{bit}$ in Fig. 2(b)). These forces done by the rock at the bit depend on the axial speed ($\dot{u}_{bit}$). Note that these forces at the bit couple axial and torsional vibrations.

### 2.4 Reduced model

Usually the final discretized FE system have big matrices (dimension $m \times m$) and the dynamic analysis may be time consuming, which is the case of the analysis presented. One way to reduce the system is to project the nonlinear dynamical equation on a subspace $V_n \in \mathbb{R}^m$, with $n << m$. In this paper, the basis used to generate $V_n$ for the reduction basis is formed by the normal modes, but, as it will be pointed out later, these normal modes have to properly be chosen (they can not be taken simply in the order that they appear). The normal modes are obtained from the following generalized eigenvalue problem,

$$([K] + [K_f] + [K_g(\mathbf{u}_S)])\boldsymbol{\phi} = \omega^2([M] + [M_f])\boldsymbol{\phi} \,, \tag{17}$$

where $\boldsymbol{\phi}_i$ is the $i$-th normal mode and $\omega_i$ is the $i$-th natural frequency. Using the representation

$$\bar{\mathbf{u}} = [\Phi]\,\mathbf{q}\,, \tag{18}$$

and substituting it in the equation of motion yield

$$([M]+[M_f])[\Phi]\ddot{\mathbf{q}}+([C]+[C_f])[\Phi]\dot{\mathbf{q}}+([K]+[K_f]+[K_g(\mathbf{u}_S)])[\Phi]\mathbf{q} = \bar{\mathbf{f}}_{NL}(t,\bar{\mathbf{u}},\dot{\bar{\mathbf{u}}},\ddot{\bar{\mathbf{u}}})\,. \tag{19}$$

where $[\Phi]$ is a $(m \times n)$ real matrix composed by $n$ normal modes obtained using the prestressed configuration. Projecting the equation on the subspace spanned by these normal modes yields

$$\begin{aligned}&[\Phi]^T([M]+[M_f])[\Phi]\ddot{\mathbf{q}} + [\Phi]^T([C]+[C_f])[\Phi]\dot{\mathbf{q}}+\\ &+[\Phi]^T([K]+[K_f]+[K_g(\mathbf{u}_S)])[\Phi]\mathbf{q} = [\Phi]^T\bar{\mathbf{f}}_{NL}(t,\bar{\mathbf{u}},\dot{\bar{\mathbf{u}}},\ddot{\bar{\mathbf{u}}})\ ,\end{aligned} \tag{20}$$

which can be rewritten as

$$[M_r]\,\ddot{\mathbf{q}}(t) + [C_r]\,\dot{\mathbf{q}}(t) + [K_r]\,\mathbf{q}(t) = [\Phi]^T\bar{\mathbf{f}}_{NL}(t,\bar{\mathbf{u}},\dot{\bar{\mathbf{u}}},\ddot{\bar{\mathbf{u}}})\,, \tag{21}$$

in which

$$[M_r] = [\Phi]^T([M]+[M_f])[\Phi], \quad [C_r] = [\Phi]^T([C]+[C_f])[\Phi]$$

$$[K_r] = [\Phi]^T([K]+[K_f]+[K_g(\mathbf{u}_S)])[\Phi] \tag{22}$$

are the reduced matrices.

## 3 PROBABILISTIC MODEL OF THE BIT-ROCK INTERACTION MODEL

Figure 3 shows a general system with a local nonlinearity. We should identify the local nonlinear operator (which, in the present case, is the nonlinear operator of the bit-rock interaction model) and then construct a probability density function for it. Note that the operator changes with time, but this is not a problem for the strategy adopted.

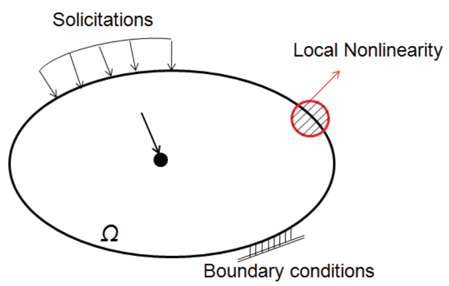


Figure 3: Local nonlinearity.

The parametric probabilistic approach allows physical parameter uncertainties to be modeled. It should be noted that the underlying deterministic model defined by Eq. (15) exhibits parameters ($a_1$, $a_2$, $a_3$, $a_4$ and $a_5$) which are obtained by an identification process, so it would be difficult to propose a stochastic model for each one, moreover they are not independent from each other. We then proposed to use the nonparametric probabilistic approach of uncertainties

[19] consisting in globally modeling the operator of the constitutive equation, Eq. (15), by a random operator.

In the early works, the nonparametric probabilistic approach was applied for linear operators [21]. Recently is was extended to geometrically nonlinear dynamical systems [11], but the type of problem studied here is completely different. We are dealing with a nonlinear operator that is an interaction model (bit-rock interaction), therefore it requires a different methodology, and we propose to use the nonparametric idea.

For convenience Eq. (15) is rewritten in the matrix form as

$$\mathfrak{f}_{bit}(\dot{\mathbf{x}}) = -[A_b(\dot{\mathbf{x}})]\dot{\mathbf{x}}\,, \tag{23}$$

in which $[A_b(\dot{\mathbf{x}})]$ is the positive-definite matrix depict by:

$$[A_b(\dot{\mathbf{x}})] = \begin{pmatrix} \left(\dfrac{a_1}{a_2\dot{u}_{bit}} + \dfrac{1}{a_2 Z(\dot{\theta}_{bit})^2} - \dfrac{a_3\dot{\theta}_{bit}}{a_2 Z(\dot{\theta}_{bit})\dot{u}_{bit}}\right) & 0 \\ 0 & \left(\dfrac{a_4 Z(\dot{\theta}_{bit})^2\dot{u}_{bit}}{\dot{\theta}_{bit}^2} + \dfrac{a_5 Z(\dot{\theta}_{bit})}{\dot{\theta}_{bit}}\right) \end{pmatrix}, \tag{24}$$

and

$$\mathfrak{f}_{bit}(\dot{\mathbf{x}}) = \begin{pmatrix} f_{bit} \\ t_{bit} \end{pmatrix} \quad \text{and} \quad \dot{\mathbf{x}} = \begin{pmatrix} \dot{u}_{bit} \\ \dot{\theta}_{bit} \end{pmatrix}.$$

The final form of $[A_b(\dot{\mathbf{x}})]$ is not obvious, but analyzing the virtual power of the system, which can be written as:

$$\delta\mathcal{P}_{bit}(\dot{\mathbf{x}}) = \;< \mathfrak{f}_{bit}(\dot{\mathbf{x}}), \delta\dot{\mathbf{x}} > \;=\; < -[A_b(\dot{\mathbf{x}})]\dot{\mathbf{x}}, \delta\dot{\mathbf{x}} >\,, \tag{25}$$

we see that to recover the force $\mathfrak{f}_{bit}(\dot{\mathbf{x}})$ one should do:

$$\mathfrak{f}_{bit}(\dot{\mathbf{x}}) = \nabla_{\delta\dot{\mathbf{x}}}\,\delta\mathcal{P}_{bit}(\dot{\mathbf{x}})\,, \tag{26}$$

$$\mathfrak{f}_{bit}(\dot{\mathbf{x}}) = -[A_b(\dot{\mathbf{x}})]\dot{\mathbf{x}} = -\begin{pmatrix} \dfrac{a_1}{a_2} + \dfrac{\dot{u}_{bit}}{a_2 Z(\dot{\theta}_{bit})^2} - \dfrac{a_3\dot{\theta}_{bit}}{a_2 Z(\dot{\theta}_{bit})} \\ \dfrac{a_4 Z(\dot{\theta}_{bit})^2\dot{u}_{bit}}{\dot{\theta}_{bit}} + a_5 Z(\dot{\theta}_{bit}) \end{pmatrix}. \tag{27}$$

To verify the positive-definiteness of $[A_b(\dot{\mathbf{x}})]$, in our case, we simply check if the diagonal terms are greater than zero, and this is true for the range of values that we are working with.

The nonparametric probabilistic approach consists, for all deterministic vector $\dot{\mathbf{x}}$, in modeling the matrix $[A_b(\dot{\mathbf{x}})]$ by a random matrix $[\mathbf{A}_b(\dot{\mathbf{x}})]$ with values in the set $\mathbb{M}_n^+(\mathbb{R})$ of all positive-definite symmetric $(n \times n)$ real matrices, with $n = 2$. Note that for each instant the matrix $[\mathbf{A}_b(\dot{\mathbf{x}})]$ will be different because it depends on $\dot{\mathbf{x}}$ that changes with time.

In order to apply the nonparametric probabilistic approach for the operator $[A_b(\dot{\mathbf{x}})]$, we have to define the available information and in a second step construct the probability density function of the random matrix using the Maximum Entropy Principle. The available information is made up of

1. $\forall\, \dot{\mathbf{x}}$, random matrix $[\mathbf{A}_b(\dot{\mathbf{x}})]$ is positive definite almost surely,
2. $E\{[\mathbf{A}_b(\dot{\mathbf{x}})]\} = [A_b(\dot{\mathbf{x}})]$ ,
3. $E\{||[\mathbf{A}_b(\dot{\mathbf{x}})]^{-1}||_F^2\} = \mathrm{c}_1$ , $|\mathrm{c}_1| < +\infty$ ,

in which $E\{\cdot\}$ is the mathematical expectation, $||\cdot||_F$ denotes the Frobenius norm of the matrix ($||[B]||_F = (tr\{[B][B]^T\})^{1/2}$) and $[A_b(\dot{\mathbf{x}})]$ is the matrix of the mean model. Following the methodology of the nonparametric probabilistic approach, the mean value is written, using the Cholesky decomposition, as

$$[A_b(\dot{\mathbf{x}})] = [L_b(\dot{\mathbf{x}})]^T [L_b(\dot{\mathbf{x}})]\,, \tag{28}$$

and the random matrix $[\mathbf{A}_b(\dot{\mathbf{x}})]$ is defined by

$$[\mathbf{A}_b(\dot{\mathbf{x}})] = [L_b(\dot{\mathbf{x}})]^T [\mathbf{G}_b][L_b(\dot{\mathbf{x}})]\,. \tag{29}$$

In the above equation, $[\mathbf{G}_b]$ is a random matrix satisfying the following available information,

1. random matrix $[\mathbf{G}_b]$ is positive definite almost surely,
2. $E\{[\mathbf{G}_b]\} = [\,I\,]$ ,
3. $E\{||[\mathbf{G}_b]^{-1}||_F^2\} = \mathrm{c}_2$ , $|\mathrm{c}_2| < +\infty$ ,

in which $[\,I\,]$ is the identity matrix. It should be noted that, in this construction, the random matrix $[\mathbf{G}_b]$ neither depends on $\dot{\mathbf{x}}$ nor on time. Taking into account the available information and applying the Maximum Entropy Principle yields an explicit expression [20] of the probability density function $p_{[\mathbf{G}_b]}$ which is written as

$$p_{[\mathbf{G}_b]}([G_b]) = \mathbb{1}_{\mathbb{M}_n^+(\mathbb{R})}([G_b]) C_{\mathbf{G}_b} det([G_b])^{(n+1)\frac{(1-\delta^2)}{2\delta^2}} \exp\left\{-\frac{(n+1)}{2\delta^2} tr[G_b]\right\}, \tag{30}$$

in which $det(\cdot)$ is the matrix determinant, $tr(\cdot)$ is the matrix trace and $\delta$ is the dispersion parameter of the distribution. The constant of normalization is written as

$$C_{\mathbf{G}_b} = \frac{(2\pi)^{-n(n-1)/4}\left(\frac{n+1}{2\delta^2}\right)^{n(n+1)(2\delta^2)^{-1}}}{\left\{\prod_{j=1}^{n}\Gamma\left(\frac{n+1}{2\delta^2}+\frac{1-j}{2}\right)\right\}}\,, \tag{31}$$

where $\Gamma(z)$ is the gamma function defined for $z > 0$ by $\Gamma(z) = \int_0^{+\infty} t^{z-1}e^{-t}dt$ and the dispersion parameter $\delta$ is given by

$$\delta = \left\{\frac{1}{n} E\{||[\mathbf{G_b}] - [I]||_F^2\}\right\}^{\frac{1}{2}}\,. \tag{32}$$

The random generator of independent realizations of random matrix $[\mathbf{G}_b]$, for which the probability density function is defined by Eq. (30), is given in appendix A. Attention with the stochastic solver because while matrix $[A_b(\dot{\mathbf{x}})]$ changes with time, random matrix $[\mathbf{G}_b]$ is constant in time.

In the deterministic equation, we have

$$\mathcal{L}_{NL}(\overline{\mathbf{u}}(t), \dot{\overline{\mathbf{u}}}(t), \ddot{\overline{\mathbf{u}}}(t)) = \mathbf{f}_{br}(\dot{\overline{\mathbf{u}}}(t))\,, \tag{33}$$

where $\mathcal{L}_{NL}$ represents all the terms in Eq. (8) except the bit forces $\mathbf{f}_{br}$. The only nonzero components of $\mathbf{f}_{br}$ are related to the axial and torsional d.o.f. at $x = L$, which are represented by $\mathfrak{f}_{bit}$, Eq. (23). For the stochastic equation, we have

$$\mathcal{L}_{NL}(\overline{\mathbf{U}}(t), \dot{\overline{\mathbf{U}}}(t), \ddot{\overline{\mathbf{U}}}(t)) = \mathbf{F}_{br}(\dot{\overline{\mathbf{U}}}(t)) \,, \tag{34}$$

where $\overline{\mathbf{U}}(t)$ is the random response and $\mathbf{F}_{br}$ is the random force at the bit for which the only nonzero components are related to the axial and torsional d.o.f. at $x = L$. This force is $\mathfrak{F}_{bit}$ which is the random variable related to $\mathfrak{f}_{bit}$ and is written as $\mathfrak{F}_{bit} = [L_b(\dot{\mathbf{x}})]^T [\mathbf{G}_b][L_b(\dot{\mathbf{x}})]\dot{\mathbf{x}}$. Let

$$[\mathbf{G}_b(s_1)], \ldots, [\mathbf{G}_b(s_\nu)] \tag{35}$$

be $\nu$ independent realizations of random matrix $[\mathbf{G}_b]$. For each realization $s_j$, we have to solve the deterministic equation

$$\mathcal{L}_{NL}(\overline{\mathbf{U}}(t, s_j), \dot{\overline{\mathbf{U}}}(t, s_j), \ddot{\overline{\mathbf{U}}}(t, s_j)) = \mathbf{F}_{br}(\dot{\overline{\mathbf{U}}}(t, s_j)) \,. \tag{36}$$

Two probabilistic models are then analyzed.

(1) Nonparametric probabilistic model

In the nonparametric probabilistic model presented above there are statistical coupling terms induced by the model uncertainties and the random matrix $[\mathbf{G}_b]$ is written as:

$$[\mathbf{G}_b] = \begin{pmatrix} [\mathbf{G}_b]_{11} & \zeta \\ \zeta & [\mathbf{G}_b]_{22} \end{pmatrix} \tag{37}$$

where $\zeta = [\mathbf{G}_b]_{21} = [\mathbf{G}_b]_{12}$.

(2) Approximation without the statistical coupling terms

What is called here the non-coupled probabilistic model is the previous model without the extra coupling terms that appear in the extra-diagonal elements ($\zeta = 0$). The idea is not to randomize all the operator, but to investigate how a global change in the parameters affects the system response. To do so, we simply set the extra-diagonal terms of $[\mathbf{G}_b]$ equal to zero,

$$[\mathbf{G}_b] = \begin{pmatrix} [\mathbf{G}_b]_{11} & 0 \\ 0 & [\mathbf{G}_b]_{22} \end{pmatrix} . \tag{38}$$

Doing so, there is no extra coupling between $\dot{u}_{bit}$ and $\dot{\theta}_{bit}$. But note that even in the deterministic system $\dot{u}_{bit}$ depends on $\dot{\theta}_{bit}$ and vice-versa.

## 4 NUMERICAL RESULTS

The drill-string was discretized using $56$ finite elements. For the dynamics analysis it was used $10$ lateral modes, $10$ torsional modes, $10$ axial modes and also the two rigid body modes of the structure (axial and torsional), so matrix $[\Phi]$ is composed by $32$ modes. For the time integration procedure, a scheme based on the Newmark method has been implemented with a procedure to equilibrate the system response in each time step. The system parameters used are representative values that are found in the literature [2, 26, 7], see appendix B.

### 4.1 Deterministic response

Fig. 4 shows a comparison of the dynamic response with and without the fluid-structure interaction.

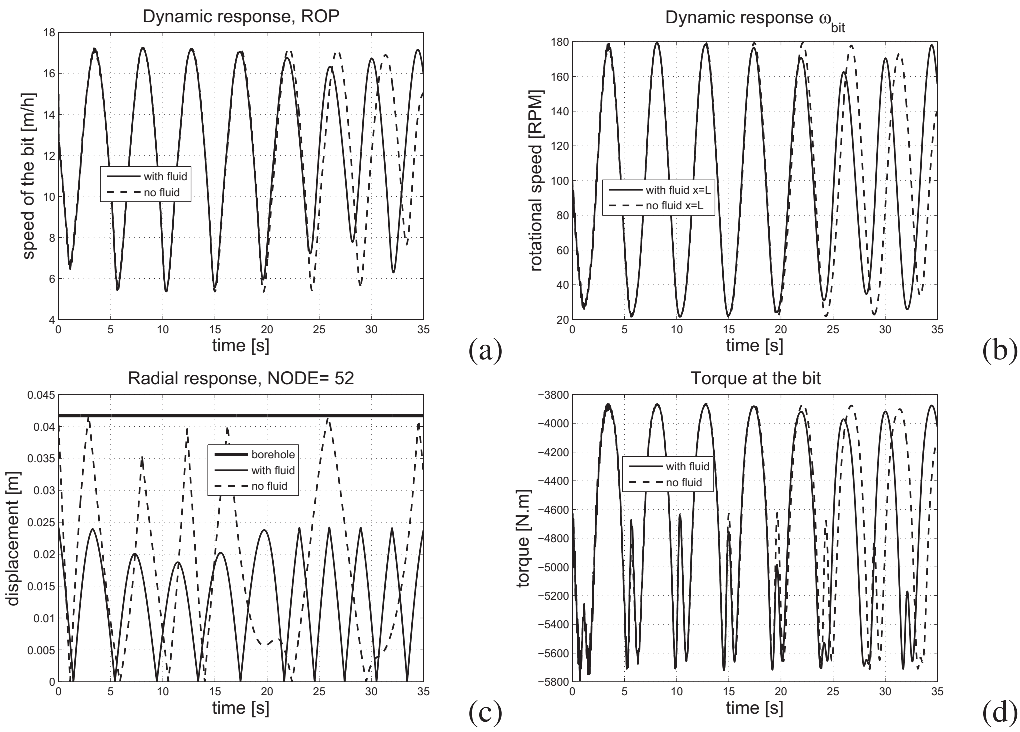


Figure 4: Response with fluid $\times$ without fluid. (a) axial speed at $x = L$, or rate of penetration (ROP); (b) rotation speed at $x = L$ ($\omega_{bit}$); (c) radial displacement at $x = 1560$ m; and (d) torque at the bit.

The main difference in the dynamic response with and without the fluid-structure interaction model is in the lateral dynamic response, see Fig. 4(c). The model used for the fluid has a major influence in the lateral frequencies and lateral mode shapes, but the axial and torsional frequencies are unaffected, which is not a surprise since in the formulation used (see Section 2.2) the axial movement is only affected by a constant force $\mathbf{f}_f$. However, the dynamics is nonlinear and the vibrations are all coupled, see that after 20 seconds of simulation the two dynamics (with and without fluid) separate. Comparing the lateral vibration, in a general way (see Fig. 4(c)), the amplitude of vibration in the BHA region is smaller when the fluid is considered because the lateral stiffness of the system increase in the presence of the fluid.

Fig. 4 (a) shows the ROP which is can be taken as a measure of the performance of the system. In a drilling operation we want to maximize the ROP to minimize the drilling time, since the ROP is inversely proportional to the well cost (the higher the ROP the lower the cost). Fig. 4 (b) and (d) shows the self excited response os the system which has a dominant frequency of $0.22$ Hz. This frequency is a little higher than the first torsional natural frequency which is $0.21$ Hz.

### 4.2 Stochastic analysis using the non-coupled nonparametric probabilistic model

Fig. 5 shows 50 Monte Carlo simulations and the $95\%$ envelope (that is to say the confidence region constructed with a probability level of 0.95) for the rate-of-penetration using a small dispersion parameter $\delta = 0.01$. The envelopes (the upper and lower envelopes of the confidence region) are calculated using the method of quantiles [24].

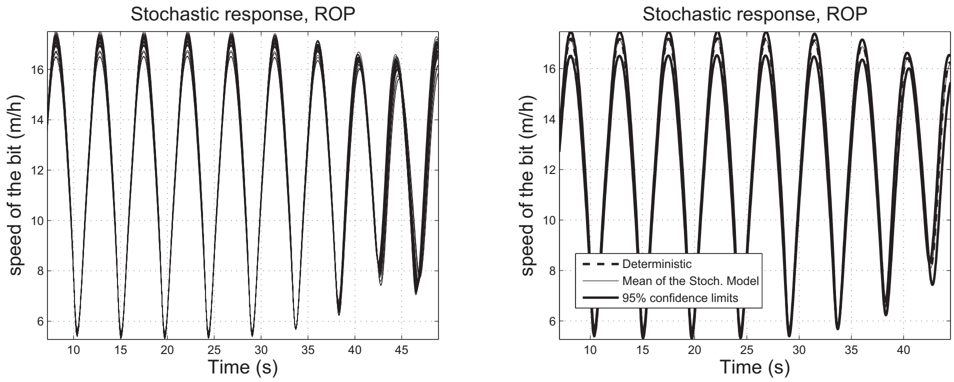


Figure 5: $\delta = 0.01$. Rate-of-penetration, ROP, for the non-coupled stochastic model. Left: 50 Monte Carlo simulations. Right: $95\%$ envelope.

Fig. 6 shows the stochastic response of the rotation speed of the bit.

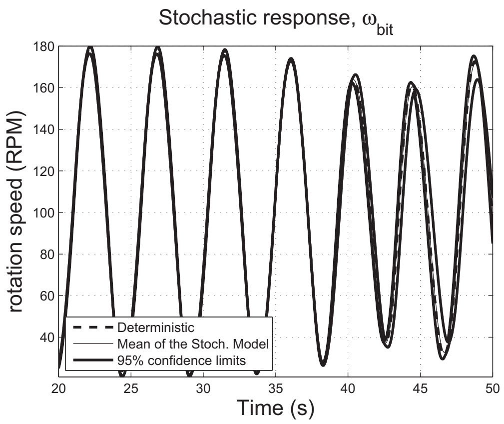


Figure 6: $\delta = 0.01$. Non-coupled stochastic model, $95\%$ envelope of the rotation speed of the bit.

It is noted that for $\delta = 0.01$ the response does not change much (see that how thin is the envelope), therefore $\delta$ will be increased in the next analysis. Fig. 7 shows the 50 Monte Carlo simulations for $\delta = 0.3$.

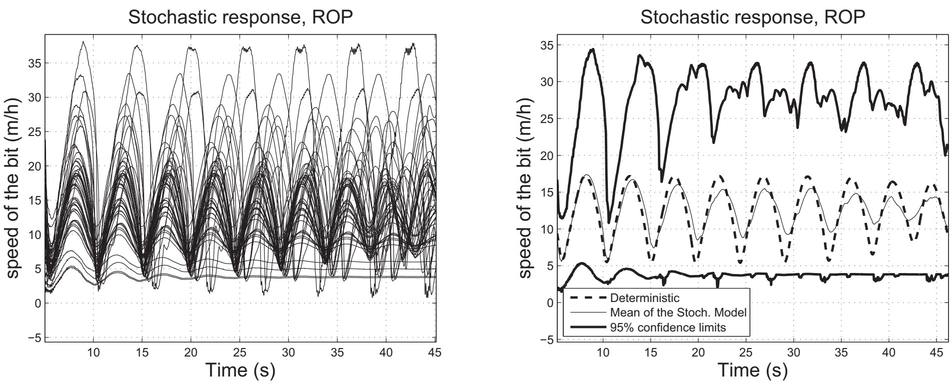


Figure 7: $\delta = 0.3$. Non-coupled stochastic model. Left: stochastic responses of the ROP. Right: $95\%$ envelope.

Note that the response envelope is thicker than as before. In the deterministic analysis the average ROP was around 11 m/h, but in the stochastic analysis the average ROP can vary from 5 to 18 m/h, which is a significant difference.

It can be concluded that the bit-rock model used is robust for changes in the parameters because the response follows the same pattern even for $\delta = 0.3$. So, this model can be used for different rock properties, or for different cutting characteristics of the bit, for instance.

### 4.3 Stochastic analysis using the usual nonparametric probabilistic model

Now lets analyze the results using the usual nonparametric probabilistic model. Fig. 8 shows 50 Monte Carlo simulations and the $95\%$ envelope for the nonparametric model using $\delta = 0.01$.

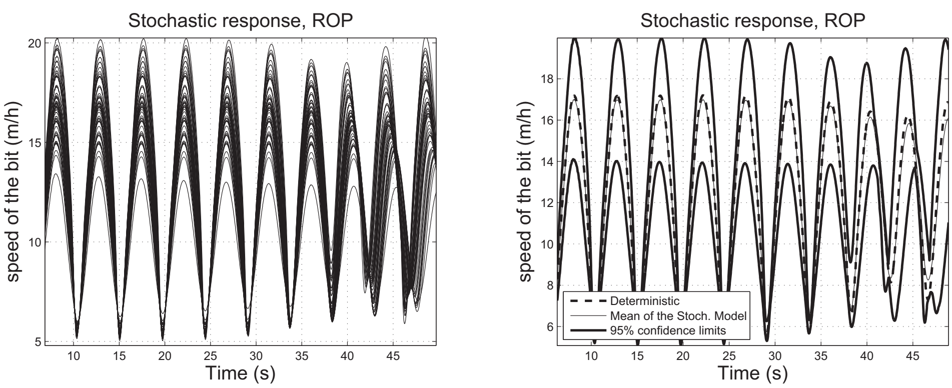


Figure 8: $\delta = 0.01$. Nonparametric model, rate-of-penetration, ROP. Left: 50 Monte Carlo simulations. Right: $95\%$ envelope.

Fig. 9 shows the $95\%$ envelope of the rotation speed of the bit using $\delta = 0.01$.

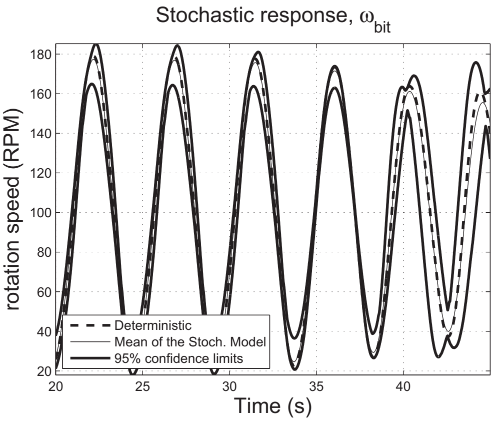


Figure 9: $\delta = 0.01$. Nonparametric model, rotation speed of the bit, $95\%$ envelope.

Note that even for a small dispersion, $\delta = 0.01$, the stochastic response presents a significative variance. The probability space is richer when the usual nonparametric model is used, *i.e.*, there is an extra coupling and model uncertainties are taken into account. The dispersion will be increased to verify the robustness of the bit-interaction model to model uncertainties, Fig. 10.

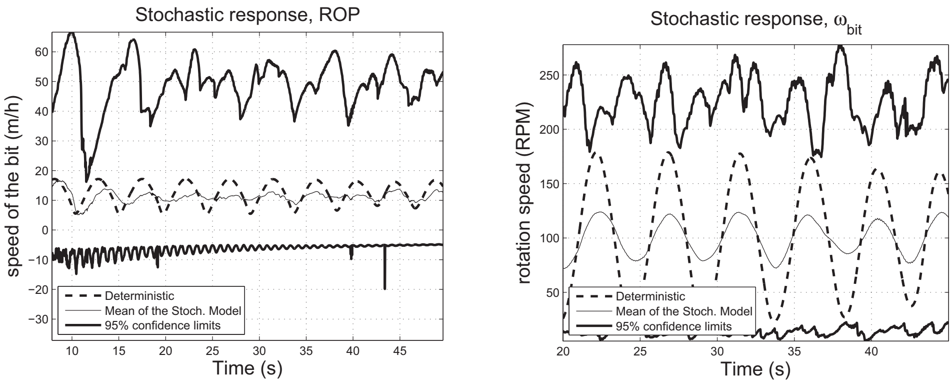


Figure 10: $\delta = 0.1$. Nonparametric model, $95\%$ envelope. Left: rate-of-penetration, ROP. Right: rotation speed of the bit.

Fig. 10 shows that there are some realizations that present negative rate-of-penetration. See Fig. 11, where 50 Monte Carlo simulations for $\delta = 0.03$ are plotted.

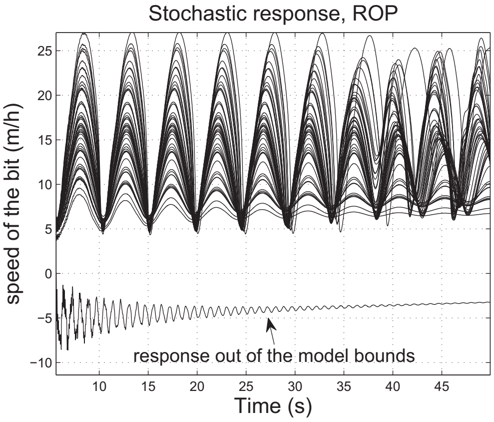


Figure 11: $\delta = 0.03$. Nonparametric model. 50 Monte Carlo simulations of the ROP.

When the complete nonparametric model is used, there are some realizations (the ones in the bottom of Fig. 11) that escape the limits of the model we are working with because the bit loses contact with the soil. The bit-bounce phenomenon is not considered in the current model.

We may say then that the bit-rock interaction model, although robust to parameters change, is not robust to model uncertainties. Using the complete nonparametric model, a little perturbation in the operator related to the bit-rock interaction ($\delta = 0.03$) leads to a stochastic response with large confidence region and there are some dynamic responses that get out of the model's bound.

## 5 CONCLUSIONS

A probabilistic model was proposed to model uncertainties for local nonlinearities. The local nonlinearity considered was the bit-rock interaction of a drill-string dynamics. The uncertain numerical model showed to be well suited. As the parameters of the bit-rock interaction do not correspond to physical parameters, it can easily be concluded that it is not really adequate to use the parametric probabilistic approach to model the uncertainties, therefore the nonparametric probabilistic approach is used. This corresponds to a completely novel approach to take into account model uncertainties in a nonlinear constitutive equation. Since the dynamical system is globally nonlinear, an adapted strategy is developed to implement the stochastic simulation. The results showed that when no extra coupling is included in the stochastic model (*i.e.*, when only the parameters are changed) the bit-rock interaction model is robust to uncertainties, but when the extra coupling is considered (*i.e.*, when the model is changed), a small uncertainty leads to a very spread response and there are some realizations that get out of the model's bound. This means that this bit-rock interaction model should be used in situations close to the stable one because it was seen that it is very sensitive to model uncertainties.

The Timoshenko beam model is used and the main forces that affect the dynamics are considered: motor torque (as a constant rotation speed at the top), supporting force, stabilizers, bit-rock interaction that describes the rate-of-penetration, impact and rubbing between the column and the borehole, fluid-structure interaction (that flows downwards then goes upwards). Finite deformations were considered without neglecting the higher order terms and the vibration was computed about a prestressed configuration.

## ACKNOWLEDGEMENTS

The authors acknowledge the financial support of CNPQ, CAPES and FAPERJ.

## A Algorithm for the realizations of the random germ $[\mathbf{G}]$

Random matrix $[\mathbf{G}]$ can be written as $[\mathbf{G}] = [\mathbf{L}_G]^T[\mathbf{L}_G]$ in which $[\mathbf{L}_G]$ is an upper triangular real random matrix such that:

1. The random variables $\{[\mathbf{L}_G]_{jj'}, j \leq j'\}$ are independents.

2. For $j < j'$ the real-valued random variable $[\mathbf{L}_G]_{jj'} = \sigma V_{jj'}$, in which $\sigma = \delta(n+1)^{-1/2}$ and $V_{jj'}$ is a real-valued gaussian random variable with zero mean and unit variance.

3. For $j = j'$ the real-valued random variable $[\mathbf{L}_G]_{jj} = \sigma(2V_j)^{1/2}$. In which $V_j$ is a real-valued gamma random variable with probability density function written as
$p_{V_j}(v) = \mathbb{1}_{\mathbb{R}^+}(v)\, \frac{1}{\Gamma\left(\frac{n+1}{2\delta^2}+\frac{1-j}{2}\right)}\; v^{\frac{n+1}{2\delta^2}-\frac{1+j}{2}}\; e^{-v}.$

## B Data used in the simulation

$\Omega_x = 100$ [RPM] (imposed rotational speed about $x$-axis at $x = 0$ m), $f_c = 100$ [kN] (initial reaction force at the bit), $L_{dp} = 1400$ [m] (length of the drill pipe), $L_{dc} = 200$ [m] (length of the drill collar), $D_{odp} = .127$ [m] (outside diameter of the drill pipe), $D_{odc} = .2286$ [m] (outside diameter of the drill collar), $D_{idp} = .095$ [m] (inside diameter of the drill pipe), $D_{idc} = 0.0762$ [m] (inside diameter of the drill collar), $D_{ch} = 0.3$ [m] (diameter of the borehole (channel)), $x_{stab} = 1400$ [m] (location of the stabilizer), $k_{stab} = 17.5$ [MN/m] (stiffness of the stabilizer per meter), $E = 210$ [GPa] (elasticity modulus of the drill string material), $\rho = 7850$ [kg/m$^3$] (density of the drill string material), $\nu = .29$ [-] (poisson coefficient of the drill string material), $k_s = 6/7$ [-] (shearing correcting factor), $c_1 = 0.01$ [N.s/m] (friction coefficient for the axial rigid body motion), $c_2 = 0.01$ [N.s/m] (friction coefficient for the rotation rigid body motion), $k_{ip} = 1e8$ [N/m] (stiffness per meter used for the impacts), $\mu_{ip} = 0.0005$ [-] (friction coefficient between the string and the borehole), $u_{in} = 1.5$ [m/s] (flow speed in the inlet), $\rho_f = 1200$ [kg/m$^3$] (density of the fluid), $C_f = .0125$ [-] (fluid viscous damping coefficient), $k = 0$ [-] (fluid viscous damping coefficient), $g = 9.81$ [m/s$^2$] (gravity acceleration), $a_1 = 3.429e-3$ [m/s] (constant of the bit-rock interaction model), $a_2 = 5.672e-8$ [m/(N.s)] (constant of the bit-rock interaction model), $a_3 = 1.374e-4$ [m/rd] (constant of the bit-rock interaction model), $a_4 = 9.537e6$ [N.rd] (constant of the bit-rock interaction model), $a_5 = 1.475e3$ [N.m] (constant of the bit-rock interaction model), $e = 2$ [rd/s] (regularization parameter). The damping matrix is constructed using the relationship $[C] = \alpha([M] + [M_f]) + \beta([K] + [K_f] + [K_g(\mathbf{u}_S)])$ with $\alpha = .01$ and $\beta = .0003$.

## REFERENCES


[1] ASME, *Handbook: Drilling fluids processing*. Elsevier, Inc., 2005.

[2] A. P. Christoforou, A. S. Yigit, Fully vibrations of actively controlled drillstrings. *Journal of Sound and Vibration*, **267**, 1029–1045, 2003.

[3] P. Coussot, F. Bertrand, B. Herzhaft, Rheological Behavior of drilling muds, characterization using MRI vizualization. *Oil and Gas Science and Technology*, **59(1)**, 23–29, 2004.

[4] M. P. Escudier, P. J. Oliveira, F. T. Pinho, Fully developed laminar flow of purely viscous non-Newtonian liquids through annuli, including the effects of eccentricity and inner-cylinder rotation. *International Journal of Heat and Fluid Flow*, **23**, 52–73, 2002.

[5] E. Jaynes, Information theory and statistical mechanics. *The Physical Review*, **106(4)**, 1620–630, 1957.

[6] E. Jaynes, Information theory and statistical mechanics II. *The Physical Review*, **108**, 171–190, 1957.

[7] Y.A. Khulief , F. A. Al-Sulaiman, S. Bashmal, Vibration analysis of drillstrings with self excited stick-slip oscillations. *Journal of Sound and Vibration*, **299**, 540–558, 2007.

[8] K. A. Macdonald, J. V. Bjune, Failure analysis of drillstrings. *Engineering Failure Analysis*, **14**, 1641–1666, 2007.

[9] M. P. Mignolet, C. Soize, Nonparametric Stochastic Modeling of Structural Dynamic Systems with Uncertain Boundary Conditions. *9th U.S. National Congress on Computational Mechanics*, San Francisco, US, Jul. 23-26, 2007.

[10] M. P. Mignolet, C. Soize, Uncertain coupling between substructures: a nonparametric Stochastic Modeling. *8th. World Congress on Computational Mechanics (WCCM8)*, Venice, Italy, Jun. 30 Jul. 5., 2008.

[11] M. P. Mignolet, C. Soize, Stochastic Reduced Order Models For Uncertain Geometrically Nonlinear Dynamical Systems. *Computer Methods in Applied Mechanics and Engineering*, **197(45-48)**, 3951–3963, 2008.

[12] M. P. Paidoussis, T. P. Luu, S. Prabhakar, Dynamics of a long tubular cantilever conveying fluid downwards, which then flows upwards around the cantilever as a confined annular flow. *Journal of Fluids and Structures*, **24(1)**, 111–128, 2007.

[13] E. P. F. Pina, M. S. Carvalho, Three-Dimensional Flow of a Newtonian Liquid Through an Annular Space with Axially Varying Eccentricity. *Journal of Fluids Engineering*, **128(2)**, 223–231, 2006.

[14] T. G. Ritto, R. Sampaio, C. Soize, Drill-string dynamics coupled with the drilling fluid dynamics. *Proceedings of the XIII DINAME, Angra dos Reis, RJ*, Rio de Janeiro, Brazil, Mar. 2 6, 2009.

[15] R. Sampaio, S. Bellizzi, POMs analysis of randomly vibrating systems obtained from Karhunen-Loève expansion. *Journal of Sound and Vibration*, **297**, 774–793, 2006.

[16] R. Sampaio, M. T. Piovan, G. V. Lozano, Coupled axial/torsional vibrations of drilling-strings by mean of nonlinear model. *Mechanics Research Comunications*, **34(5-6)**, 497–502, 2007.

[17] R. Sampaio, C. Soize, On measures of nonlinearity effects for uncertain dynamical systems - Application to a vibro-impact system. *Journal of Sound and Vibration*, **303**, 659–674, 2007.

[18] C. E. Shannon, A mathematical theory of communication. *Bell System Tech. J.*, **27**, 379-423 and 623-659, 1948.

[19] C. Soize, A nonparametric model of random uncertities for reduced matrix models in structural dynamics. *Probabilistic Engineering Mechanics*, **15**, 277–294, 2000.

[20] C. Soize, Maximum entropy approach for modeling random uncertainties in transient elastodynamics. *Journal of the Acoustical Society of America*, **109(5)**, 1979–1996, 2001.

[21] C. Soize, Random matrix theory for modeling uncertainties in computational mechanics. *Computer Methods in Applied Mechanics and Engineering*, **194(12-16)**,1333–1366, 2005.

[22] P. D. Spanos, A. K. Sengupta, R. A. Cunningham, P. R. Paslay, Modeling of roller cone bit lift-off dynamics in rotary drilling. *Journal of Energy Resources Technology*, **117(3)**, 197–207, 1995.

[23] P. D. Spanos, A. M. Chevallier, N. P. Politis, M. L. Payne, Oil and Gas Well Drilling: A Vibrations Perspective. *The Shock and Vibration Digest*, **35(2)**, 85–103, 2003.

[24] R. J. Serfling, *Approximation Theorems of Mathematical Statistics*. John Wiley and Sons, 1980.

[25] M. A. Trindade, C. Wolter, R. Sampaio, Karhunen–Loève decomposition of coupled axial/bending of beams subjected to impacts. *Journal of Sound and Vibration*, **279**, 1015–1036, 2005.

[26] R. W. Tucker, C. Wang, Torsional vibration control and cosserat dynamics of a drill-rig assembly. *Meccanica*, **38(1)**, 143–159, 2003.